Cone penetration testing in thinly inter-layered soils

Van Der Linden, Toon I.; De Lange, Dirk A.; Korff, Mandy

DOI
10.1680/jgeen.17.00061

Publication date
2018

Document Version
Accepted author manuscript

Published in
Proceedings of the Institution of Civil Engineers: Geotechnical Engineering

Citation (APA)
Van Der Linden, T. I., De Lange, D. A., & Korff, M. (2018). Cone penetration testing in thinly inter-layered soils. *Proceedings of the Institution of Civil Engineers: Geotechnical Engineering*, *171*(3), 215-231. https://doi.org/10.1680/jgeen.17.00061

Title “Cone penetration testing in thinly inter-layered soils”

T.I. van der Linden

- Royal HaskoningDHV, *Amersfoort, The Netherlands*
- Former Department of Geo-Engineering, Delft University of Technology, *Delft, The Netherlands*

D.A. de Lange

- Deltares, *Delft, The Netherlands*

M. Korff

- Deltares, *Delft, The Netherlands*
- Department of Geo-Engineering, Delft University of Technology, *Delft, The Netherlands*

Full contact details of corresponding author:

T.I. (Toon) van der Linden
Royal HaskoningDHV
P.O. Box 1132
3800 BC Amersfoort
The Netherlands
https://nl.linkedin.com/in/toonvanderlinden
Toon.van.der.Linden@rhdhv.com
+31 6 17 510 131/+31 88 348 1689

Abstract (150 words)

The effect of a soft layers on the cone resistance of a sand layer has been studied extensively. However, this is not the case for multi-layered deposits with many (thin) alternating soil layers. For geotechnical analyses based on CPT data it is difficult to estimate a representative value of the cone resistance when encountering alternating thin layers of clay or peat and sand. This paper presents physical modelling tests to understand the “value” of the cone resistance in thinly multi-layered soil deposits. The test results are compared with existing analytical methods. It is concluded that the characteristic resistance of the individual layers, the layer thicknesses relative to the cone diameter and the number of layers within the zone of influence of the cone affect the cone resistance in deposits containing multiple thin soil layers. Also suggestions for practical implementation are given.

Keywords

Models (physical)

Site investigation

Geotechnical engineering

List of notation

d_{cone}	Cone diameter [mm]
D_{eq}	Equivalent pile diameter [m]
H	(Thin) layer thickness [mm]
K_H	Thin layer correction factor [-]
α_p	Pile class factor [-]
β	Pile base shape factor [-]
s	Factor which accounts for cross-sectional shape of the pile base [-]
I_D	Density index [-]
Z	Depth [mm]
p_a	Atmospheric pressure [kPa]
PI	Plasticity index [%]
$q_{b;max}$	Maximum pile tip resistance [MPa]
q_c	Measured cone resistance [MPa]
q_c^*	Characteristic cone resistance [MPa]
$q_{c,norm}$	Normalised cone resistance [-]
$q_{c,char,sand}$	Characteristic cone resistance in sand [-]
$q_{c,char,clay}$	Characteristic cone resistance in clay [-]
$q_{c,max,layer}$	Maximum cone resistance in a layer [-]
c_u	Undrained shear strength [kPa]
K_0	Coefficient of lateral earth pressure [-]
K_t	Correction factor for the cone resistance in multiple thin sand layers [-]

w	Water content [-]
σ'_m	Mean effective stress [kPa]
σ'_{v0}	Initial effective vertical stress [kPa]
σ'_v	Effective vertical stress [kPa]

1. Introduction

Cone penetration testing (CPT) is widely used to determine the geotechnical engineering properties of soils and for delineating soil stratigraphy. The resolution of CPT in delineating stratigraphic layers is related to the size of the cone tip and the friction sleeve and the sample recording related to the penetration rate. A transition zone can be defined around the interface between two different soil layers, since the cone resistance will be affected by both the under- and overlying layers. The dimensions of such a transition zone are a function of the cone tip size. The CPT interpretation within these intervals holds large uncertainty, especially for deposits containing multiple thin layers, since the cone resistance will be affected by several surrounding layers.

This study focuses on the cone resistance of sand layers in so called “flaser beds”. These are sedimentary bedding patterns created when a sediment is deposited by intermittent flows, leading to alternating sand and clay layers. Such deposits exist typically in marine environments (Reineck and Wunderlich, 1968; Martin, 2000). Figure 1 shows an example of a sediment core containing such depositional features. The sand layers typically have a thickness of 5 mm to several centimetres. A CPT (Figure 2) was undertaken adjacent to this sediment core: the location of the flaser bed deposit is marked with a dashed rectangle on the CPT plot). CPT measurements were logged at 2cm intervals of penetration. Cone resistances of between 1 and 2 MPa were measured within this bed. The pore pressure deviates somewhat from the hydrostatic line and a friction ratio around 2% is found in this region. The soil is classified as clayey silt to silty clay and sandy silt to clayey silt based on Robertson (1986).

When CPT data is being used to estimate the liquefaction potential, Idriss and Boulanger (2008) note that CPT values need to be corrected for transition zones between clay and sand. Also for other applications it is conceivable that a better understanding of CPT in thinly layered soils is desired. Flaser beds can easily be mischaracterised as clean sand, which, given the low cone resistances measured, gives a false (too high) indication of the liquefaction potential. Using CPT data measured in flaser bed deposits can have implications on the determination of stress state (e.g. by using the classification method of Robertson (1990)) or the shear strength and the density index (e.g. using the method of Baldi (1986)). Current methods for correction of thin layers are based on analytical linear elastic solutions (e.g. Vreugdenhil et al., 1994; Robertson and Fear, 1995; Joer et al., 1996) or numerical analysis for single intermediate layers only (Ahmadi and Robertson, 2005).

This paper presents the results of a feasibility study undertaken to devise a correction method which will determine more realistic engineering properties of thin sand layers within thinly interlayered zones. The measured cone resistance needs to be converted to a 'clean sand' resistance, hereafter referred to as characteristic resistance. CPT has been performed in artificially constructed deposits containing multiple soil layers. The test results are compared with existing analytical solutions for this problem. Thin layers are defined as layers which are thinner than the diameter of the penetrometer.

Figure 1: Sediment core with flaser bed sedimentation between depths of 4.5 m and 6 m marked in red (vertical scale in cm)

Figure 2: Example of cone penetration results in flaser beds undertaken close to the sediment core shown in Figure 1

2. Cone penetration testing and layered soils

According to De Beer (1963) one of the most important factors that determines the magnitude of the cone resistance are the dimensions of the failure wedge around the tip during penetration. The shape and size of this wedge depend on the cone tip size, soil strength parameters and effective stresses (Prandtl 1921). For frictional materials, such as sands, the failure surfaces typically have a logarithmic spiral form, while for clays the form of the failure surface is considered to be more circular and smaller compared to surface forms in sand (Meyerhof 1951). In homogeneous soils these shapes can be distinguished well (for example Arshad et al. 2014), whereas in soils with thin alternating layers the shape of the failure surface cannot be easily differentiated. This makes qualitative determination of the cone resistance in alternating thin layers using failure surface analysis complex.

2.1 Existing physical model tests for CPTs in thinly layered soil

For sediment profiles containing sand layers with different characteristics, the effects of layering on the cone resistance has been studied extensively (Van den Berg, 1994; Joer et al., 1996; Silva and Bolton, 2004; Młynarek et al., 2012; Mo, 2014).

From tests containing two layers (clay on sand and sand on clay), Van den Berg (1994) concluded that a cone penetrating in frictional material is influenced by an underlying soft clay layer at a distance of four to five times the cone diameter. Silva and Bolton (2004) performed piezocone tests on sand samples containing layers with different grain size fractions, while having the same density index and concluded that the effect of an underlying soil layer could be identified when the cone approaches the layer boundary at a distance of three cone diameters. Xu (2007) and Xu and Lehane (2008) concluded, based on jacked pile tests in a centrifuge, that the pile base resistance is affected at a greater distance from the layer interface when the underlying layer is softer than when the underlying layer is stiffer than the considered layer. Xu

(2007) found from the tests conducted that the distance of influence varies between three and eight times the base diameter, depending on the ratio between the characteristic resistances in the stiff and soft soil layer. Also Van der Berg (1994) and Mo (2014) conclude that the size of the transition zone depends on the stiffness ratio between the layers or the density index of both layers.

Van den Berg (1994) concluded that about six to seven times the cone diameter of penetration is needed to reach the full steady state cone resistance in a frictional layer, while the research conducted by Joer et al. (1996) consisted of penetration tests in layered cemented soil surrounded by rigid boundaries, using a 3 mm diameter probe and a 10 mm diameter cone showed that a penetration of 12 times the cone diameter and 25 times the probe diameter was needed to reach the characteristic resistance. Both Xu (2007) and Van den Berg (1994) found that as the pile or cone penetrometer enters the clay layer, the cone resistance reduces rapidly to the characteristic resistance of clay.

Mo (2014) and Mo et al. (2015) performed CPT tests in two- and three-layered soil samples. In the case of a three-layer system with a single stiffer “thin” layer, it was concluded that when the density index of the “thin” layer increases, the maximum resistance measured in the thin layer becomes smaller relative to the characteristic sand resistance. This means that for thin layers the difference between the measured and the characteristic cone resistance increases with increasing density index and is not only affected by the layer thickness.

2.2 Existing work on numerical modelling of thin layers

Based on the linear elastic solution of Vreugdenhil et al. (1994), who argue that the cone resistance is affected elastically by the presence of a nearby layer, Robertson and Fear (1995) proposed the parameter K_H to correct the cone resistance to a characteristic value. The parameter K_H is defined as the factor by which the maximum measured cone resistance of a laminated layer needs to be multiplied to obtain the equivalent thick-layer cone resistance. The equation given for K_H was presented for a standard cone having a cross-sectional area of 10 cm^2. Youd and Idriss (2001) presented a range of field data related to the correction parameter K_H, from an unpublished work of Robertson and Castro, and from this proposed a more conservative equation, since the field data indicated that K_H was being overestimated. They also stated that the correction proposed by Robertson and Fear (1995) applies only to “thin” stiff layers embedded within thick soft layers.

Ahmadi and Robertson (2005) applied a numerical modelling procedure to predict the cone resistance of an intermediate sand layer embedded within soft clay. The modelling procedure was verified with published experiments from calibration chamber tests by Ahmadi (2000) and the displacement pattern obtained from the performed numerical analysis was similar to that of the experimental observations of Van den Berg (1994). Ahmadi and Robertson (2005) showed

that the in-situ stress state can have a significant effect on the cone resistance measured in a single sand layer within a soft soil. The in-situ stress state also influences the distance to the layer interface at which the cone resistance is influenced by the following layer.
Van den Berg et al. (1996) also found that the distance over which a cone is affected by a neighbouring layer depends strongly on the stiffness ratio of the two layers, based on Eulerian finite element modelling.

Walker and Yu (2010) modelled the CPT in multi-layered clays using an explicit finite element method with adaptive mesh. It was found that when a cone passes from a weak layer to a strong layer, the change in measured resistance is abrupt, whereas when the cone proceeds from a strong layer to a weak layer the penetration resistance is significantly affected on both sides of the layer interface.

Mo et al. (2017) presented results of analytical cavity expansion solutions. By first analysing two-layered models, a simple superposition method of the two-layered problem is applied to the analysis of penetration in multi-layered soils. The analysis of CPT data in two-layered soils highlights the effect of strength and stiffness on CPT measurements within the influence zones around the two-soil interface. The effect of a single thin layer was studied, and a correction factor for “thin” layers was proposed, which fitted well with field data reported in Youd and Idriss (2001).

All research mentioned here focussed on two- or three-layered systems and did not consider thin layers. Thin layers are defined as layers which have a smaller thickness than the diameter of the penetrometer. The research presented in this paper aimed to investigate thinly inter-layered soils which contain five or more alternating sand and clay layers. For multi-layer systems, it is expected that the cone resistance would be influenced by the layer thickness (relative to the cone diameter), the number of layers within the zone of influence and the characteristic cone resistances of the individual layers, which depend on *inter alia* the porosity and the stress level.

3. Physical model tests

Physical model tests were performed in order to derive and validate an analytical method which is able to translate the measured cone resistance in thin layered soil to the characteristic cone resistance, focussing on the cone resistance of the thin sand layers. Seven soil models were prepared to investigate the suitability of the proposed test set-up. CPT was performed on saturated layered soil deposits, which were artificially built up in a cylindrical container. Four different layering configurations were tested. In this paper four tests are presented, representing each of these configurations.

3.1 Test set-up

The test set-up consisted of a hydraulic plunger fixed on a reaction frame which was able to push a miniature cone into a cylinder containing the artificially built up soil deposits. The cylindrical container was built up of separate steel rings, which had an inner diameter of 600 mm. For Test 2, the container height was 1.024 m, and 1.255 m for the other tests reported in this paper. The plunger had a stroke of 1 m and the CPT was performed in the centre of the container. A cone with a diameter of 25 mm (cross-sectional area of 5 cm^2) containing a friction sleeve with a length of 94 mm and an u_2 pore pressure transducer mounted on the shoulder of the cone has been applied, to minimise possible boundary effects. This implies a container/cone diameter ratio of 24, which is in general considered to be sufficient for sands having a (relatively) low density index (Ahmadi and Robertson, 2004; Bolton et al., 1999). A displacement transducer was used to determine the penetration depth of the cone. Figure 3 shows the container and test set up for Test 7.

Figure 3: Test set-up (steel tank with sand sample, Test 7)

3.2 Soil model

Configurations

Table 1 shows the characteristic details of the selected tests. Test 2 contained a clay layer of 300 mm thickness between two sand layers each having a bulk density index of 92%. For the initial soil models a high density index was applied in the sand layers to speed up sample preparation: in this way less sample disturbance was expected due to placing of the clay layers. However, it was found that a lower density index had to be applied to the sand layers in order to avoid boundary effects. Therefore, a bulk density index of around 55% has been applied to the sand layers in the later soil models. Test 5 contained a layered unit of three clay and two sand layers, each having a thickness of 80 mm. Test 6 contained a layered unit of ten clay and nine sand layers, each 20 mm thick. The layered units were sandwiched between two sand layers having the same density index. Test 7 consisted of sand only, in order to measure the characteristic value of the sand having a density index of around 55%. Test 2 has been used to determine the characteristic value of the clay layers. Diagrams showing the sample configurations for each test are given in Figure 4.

Table 1: Sample properties of the relevant tests

Sample nr.	Details of layered unit	I_D (sand)	Comment
Test 2	One 30 cm clay layer	92%	Reference test clay
Test 5	Three 80 mm clay layers	55%	
Test 6	Ten 20 mm clay layers	55%	
Test 7	No layering	55%	Reference test sand

Figure 4: Test configurations: (a) Test 2, (b) Test 5 and (c) Test 6

Soil materials

Baskarp sand and Vingerling clay (pottery/brick clay delivered by Sibelco, type K147) were used to create the (layered) soil deposits. Table 2 and Table 3 give some characteristics of both materials. The seeving characteristics of the Baskarp sand were obtained from two resembling measurements, while the minimum and maximum void ratios were determined for multiple sand samples. For every brick of clay delivered, the undrained shear strength and water content were measured. The presented undrained shear strength has been measured by means of pocket penetrometer testing. Table 3 presents the mean value of all measurements, as well as the standard deviation (SD).

Table 2: Characteristics of Baskarp sand

	d_{50} [mm]	d_{60}/d_{10} [-]	min-max void ratio [-]
Baskarp sand	0.151	1.5	55.3% - 89.0%

Table 3: Characteristics of Vingerling clay

	c_u [kPa]	w [-]	PI [%]
Vingerling clay	15 (SD = 0.5)	24% (SD = 0.3%)	17

Figure 5: Preparation of clay layers for Test 2

Preparation method

The desired density index for the sand layers was obtained by gently pouring the sand into the container filled with water and, after that, compacting each sand layer by gentle tamping with a flat cylindrical plate (diameter 6.5 cm) until a layer thickness of 2.0 cm had been reached. The density index was determined by measuring the height of the soil model during sample preparation and the weight of the sand that had been poured into the water. In this way, saturated soil samples were created.

The Vingerling clay was delivered in bricks. To create clay layers with a certain height, the bricks were cut by a steel wire in slices and carefully laid next to each other, forming a continuous layer, on the sand surface (see Figure 5). Capillary forces were created at the sand surface level to strengthen it so as to reduce the sample disturbance due to placement of the clay slices. Further details on the preparation methods used in this research are described by De Lange et al. (2016) and Van der Linden (2016).

3.3 Test procedure

Before testing, the pore pressure filter and transducer of the CPT probe were saturated by maintaining a vacuum pressure for at least 12 hours while immersed in silicone oil. Saturated

conditions during the tests were ensured by a water level of a few centimetres above the soil surface level.

In order to obtain a sufficient level of detail, measurements taken sampled at 1 mm intervals. Since the applied data acquisition system had a maximum sampling frequency of 4 Hz, CPT was performed with a penetration rate of 4 mm/s and a sampling frequency of 4 Hz was applied. Sleeve friction and pore pressure were recorded along with cone resistance.

After performing CPT, the samples were excavated, visually inspected and photographed with the cone left in place. Samples were also taken in order to determine the local density index. Although samples taken after testing were affected by the cone penetration, the measurements give an indication of the sample homogeneity.

3.4 Test results

Cone resistance

In this section the CPT results are presented in this section. Figure 6 shows the measured cone resistances during Tests 2, 5, 6 and 7. The layered units, containing 20 mm thick or 80 mm thick clay and sand layers can be clearly distinguished in Tests 5 and 6. The characteristic clay resistance was obtained during penetration of the 300 mm clay layer in Test 2. It should be reiterated that in this model a higher density index was applied than in the other soil models. The observed variation in sand resistance is ascribed to sample heterogeneity. The cause of the sudden decrease in cone resistance at around 0.53 m depth during Test 7 is not known.

Figure 6: Measured cone resistances; note: I_D = 92% for Test 2, 55 % for the other tests

Figure 7 shows the results of Test 5, performed on the soil model containing 80 mm thick layers. The results of the reference Test 7 are included to illustrate the effect of the clay layers. The cone resistance in the 80 mm sand layers did not fully reach the characteristic resistance of the reference sand. Figure 8 shows the results of Test 6, performed on the soil model containing 20 mm thick layers. Although the thin sand layers are still visible, the contrast between the sand and clay layers is relatively small.

It was seen that the cone resistance of the reference Test 7 between depths of 0.6 m and 0.8 m was relatively low compared to values just above and below this range. It is considered that this zone may have had a lower density index locally due to the sample preparation. This was confirmed by results of density tests on samples taken after CPT testing. The cone resistance of the sand layer at a depth of 0.7 m was also found to be denser compared to other layers, while the bottom sand layer of test 6 seems to be less dense compared to the bottom sand layers of Tests 5 and 7.

From Tests 5 and 6 it was observed that the cone resistance starts to increase towards the characteristic sand resistance before the cone has passed through the bottom clay layer. It should be noted that the cone shoulder was chosen to be the reference level. The distance between the tip and the shoulder was 22 mm. Thus, during Test 6, the cone tip enters the base sand layer before the reference point enters the bottom thin clay layer. Also, since some material is pushed in front of the cone during penetration, the "sensing level" is lowered.

Figure 7: Cone resistance results for Test 5 in layered system (three clay layers, each 80 mm thick) compared with Test 7 (reference test, sand only)

Figure 8: Cone resistance results for Test 6 in layered system (ten clay layers, each 20 mm thick) compared with Test 7 (reference test, sand only).

Sleeve friction

Friction sleeve measurements and the corresponding friction ratios are presented in Figure 9 and Figure 10 respectively. The layers of Test 5 can be clearly seen in the sleeve friction and the friction ratio plots. However, these measurements did not give a reliable indication of the location of the layers in Test 6. This is due to the friction sleeve being slightly longer than the thickness of the clay layers in Test 5 but considerably longer than the thickness of the clay layers in Test 6, causing the friction sleeve to penetrate multiple layers at the same time. When using soil classification methods like that of Robertson (1990), the resulting classification will be significantly less accurate.

Figure 9: Results of friction sleeve measurements: (a) Test 2 (30 cm clay layer); (b) Test 5 (three clay layers, each 80 mm thick); (c) Test 6 (ten layers, each 20 mm thick); (d) Test 7 (sand only)

Figure 10: Friction ratio results: (a) Test 2 (30 cm clay layer); (b) Test 5 (three clay layers, each 80 mm thick); (c) Test 6 (ten layers, each 20 mm thick); (d) Test 7 (sand only)

Pore pressure

The pore water pressure was measured during penetration using the u_2 pore pressure transducer. It should be noted that a penetration rate of 4 mm/s was applied to obtain data with a high level of detail (the standard rate applied in the field is equal to 20 mm/s). Results of the pore pressure measurements are presented in Figure 11.

Figure 11: Results of pore pressure measurements: (a) Test 2 (30 cm clay layer); (b) Test 5 (three clay layers, each 80 mm thick); (c) Test 6 (ten layers, each 20 mm thick); (d) Test 7 (sand only)

In the bottom sand layer of Test 2 (see Figure 11(a)), a decrease in pore pressure was measured, which can be explained by dilative soil behaviour due to the relatively high density index. For all tests, the increase of pore pressure relative to the hydrostatic pressure started after the cone had penetrated the clay a certain distance. This is confirmed by the results of the physical modelling by Van den Berg (1994). This effect is is thought to be the result of sand being pushed in front of the cone into the clay layers, as was observed in the dismantled soil samples. Sand intrusions along the cone rod were observed in the clay layers (see Section 4). Pore pressure measurements gave a good indication of the presence of layers of different permeability. However, the thickness of the individual layers could not be determined accurately because of the soil disturbance around the cone tip. This confirms the findings of Hird et al. (2003).

Visual inspection and sampling after CPT

The soil samples were excavated and photographed after testing, as shown in Figure 12 for Tests 5 and 6. It was clearly visible that the soil below the cone tip was pushed downwards into the underlying soil layer. The patterns of soil disturbance which were found after physical testing are comparable to the patterns of disturbance found by Emmett (2005) during installation of solid cylindrical piles, although different soil types have been used.

Figure 12: Excavation along the cone rod after completion of (a) Test 5 and (b) Test 6

To check that the sand layers were uniformly prepared, samples were taken at various depths after CPT to determine the local density. However, since the sample has been disturbed by penetration of the cone, the measurements were only used as indications of local variations and relative differences in density index of the sand layers.

4. Analysis of test results

To quantify the effect of the clay layers on the measured resistance in the intermediate sand layers, a reliable approximation of the characteristic cone resistance in clean sand is needed. However, as mentioned in Section 3, some local variation in density index was observed. Therefore, the expected variation in cone resistance due to variation in density index is calculated based on methods in Lunne et al. (1997) and Senders (2010). The relationship proposed by Lunne et al. (1997) was used to calculate the clean sand resistance as a function of the vertical effective stress level and the density index. The formula proposed by Senders (2010) was used to account for the influence of the shallow failure mechanism. Combining these relationships gives:

$$q_c = 61{\sigma'_v}^{0.71} e^{2.91 I_D} \left(1 - e^{-\left(\frac{Z \quad 0.095}{d_{cone}\, {I_D}^2}\left(\frac{\sigma'_m}{p_a}\right)^{0.5}\right)}\right), \tag{1}$$

Where σ'_v is the effective vertical stress, p_a is the atmospheric pressure and σ'_m is defined as:

$$\sigma'_m = \frac{\sigma'_v \cdot (1 + 2K_0)}{3}, \tag{2}$$

Where K_0 is the coefficient of lateral earth pressure.

The variation in density index is expected to be ± ca. 10%, based on the samples taken after CPT. Figure 13 shows the approximated characteristic cone resistances for sands with a density index of 45%, 55% and 65% respectively. The results of Tests 5, 6 and 7 are plotted in the same graph. It can be concluded that the approach fits the measured data reasonably.

Figure 13: Characteristic cone resistances based on Lunne et al. (1997) and Senders (2010) for sands with density index of 45%, 55% and 65% respectively. The results of Tests 5, 6 and 7 are presented as well (dashed lines)

The correction factor for the sand layers is defined in this research as:

$$K_t = \frac{q_{c;char;sand}}{q_{c;max;layer}} \tag{3}$$

The theoretical approximation of the characteristic cone resistance for a density index of 45% and 65% at a certain stress level were used to determine upper and lower limits of the correction factor for each layer. Correction factors were also derived for a density index of 55% and based on the data of the reference test (Test 7). The correction factors derived for test 6 are plotted in Figure 14. These tended to increase when multiple layers were passed.

Figure 14: Correction factors derived for Test 6, multiple values of the characteristic cone resistance are used to account for the observed local variation in density index

The average values of the derived correction factors are plotted in Figure 15 as function of the normalized layer thickness. Correction factors higher than 1.5 are found for thin layers where the H/d_{cone} ratio is 0.8, while correction factors lower than 1.5 are found for thicker layers, having a H/d_{cone} ratio of 3.2. It should be noted that correction factors lower than 1 are not realistic.

Figure 15: Average of derived correction factors Kt as function of the normalized layer thickness H/d_{cone}, multiple values of the characteristic cone resistance are used to account for the observed local variation in density index

5. Comparison with existing analytical models

Two analytical methods have been used to simulate the experimental results: (1) the approach of Vreugdenhil et al. (1994) and (2) the Dutch method (also known as the Koppejan method) for

determination of the end bearing capacity of foundation piles. The Dutch method is described in the Dutch annex of Eurocode 7 (NEN 9997-1).

The “simple” elastic analysis proposed by Vreugdenhil et al. (1994) has been generalised for multiple layers by Joer et al. (1996). This method determines a weighted average of the shear modulus of the separate layers, dependent on the cone tip level. The distance to a layer interface determines the degree of contribution of that layer. Vreugdenhil et al. (1994) assume that the shear modulus of a layer is proportional to the characteristic cone resistance of that layer, meaning that the relative difference in shear modulus represents the relative difference in characteristic cone resistance.

The Dutch method for determination of the pile base resistance considers the variation of the cone resistance in the range of $4D_{eq}$ below and $8D_{eq}$ above the base level. This method is derived from a combination of empirical data and theoretical influence shapes. The procedure of this method is set up such that a conservative approximation of the path of least resistance will be found. The governing equation is as follows:

$$q_{b,max} = \frac{1}{2} \cdot \alpha_p \cdot \beta \cdot s \cdot \left(\frac{q_{c,I,av} + q_{c,II,av}}{2} + q_{c,III,av} \right) \quad (4)$$

The subscripts I, II and III refer to the trajectories, for which a governing cone resistance has to be determined by averaging, see Figure 16. The distance below the pile base over which averaging takes place (trajectory I and II) varies between $0.7D_{eq}$ and $4D_{eq}$, depending on the distance over which the minimum value will be met. The procedure to determine the governing cone resistance for the trajectories II and III is determined in such way that the cone resistance taken into account cannot be higher than the qc at deeper levels of these trajectories. The distance above the pile base over which averaging takes place (trajectory III) is fixed at $8D_{eq}$. The parameters α_p, β and s represent pile type factors, which have been set to 1 for this assessment.

Figure 16: Schematic of the trajectories applied in the Dutch method

Both analytical methods are compared with the test results of Tests 5 and 6. The normalized (stress independent) cone resistance has been used as input for the analytical models. Those values are derived, in line with Lunne et al. (1997), using:

$$q_{c;norm} = \frac{q_c}{{\sigma'_v}^{0.71}} \quad (5)$$

The results of test 5, 6 and 7 normalized for the in situ effective stress level are plotted in Figure 17. The characteristic value of the normalized cone resistance of the sand layers with density index of 55% is 300 (based on Lunne et al. (1997)) and the characteristic value of the clay layers is 70, based on the results of Test 2. These characteristic values can be used as input for the analytical models and are also plotted in Figure 17.

Figure 17: Test results normalized for the stress level with characteristic values for clay and sand (dashed lines)

The simulations of Tests 5 and 6 using both analytical models are given in Figure 18 and Figure 19 respectively. The simulations using the method of Vreugdenhil et al. (1994) fit the results of Test 5 reasonably. However, this method seems to be less suitable for thin layers, based on the simulation of Test 6. The individual layers are clearly visible, however, the average resistance in the thinly layered part deviates from the actual results of Test 6. Using this elastic method, it seems to be impossible to better approach the measured resistance by using the characteristic cone resistance of the individual layers as input. The Dutch method gives a reasonable fit for the clay layers of Test 5 and for the thin sand layers of Test 6. However, the method does not appear suitable to predict the resistance of the thicker interbedded sand layers of Test 5. This is because the method was developed to find the lower limit of the pile end bearing capacity.

Figure 18: Simulations of Test 5

Figure 19: Simulations of Test 6

It is believed that the procedure of the Dutch method to determine the governing resistance over trajectories II and III might be causing the bad fit for Test 5. Therefore simulations were also made where (1) $q_{c;II}$ was ignored; and (2) both $q_{c;II}$ and $q_{c;III}$ were ignored. The results of these simulations are given in Figure 20. When only the average cone resistance over trajectory I is considered, the Dutch method fits the results of Test 5 well. Simulations by the adapted Dutch method have also been performed for Test 6, as shown in Figure 21. However, to find a good fit for the thin layers in Test 6, it turns out that it is necessary to take trajectories II and III into account.

Figure 20: Simulations of Test 5 by three variants on the Dutch method: (1) the standard procedure; (2) considering only trajectories I and III and (3) considering only trajectory I

Based on the analytical simulations, it has been concluded that thin layers require a different approach than thicker interbedded layers. This finding is in line with the statement that the magnitude of the tip resistance is determined mainly by the dimensions of the failure wedge around the tip (De Beer 1963). According to Meyerhof (1951) the shape of the failure surface in

clays is more spherical and smaller compared to the shape of the failure surface in sands. The elastic approach of Vreugdenhil et al. (1994) seems to be unsuitable for thinly layered soil deposits.

Figure 21: Simulations of Test 6 by three variants on the Dutch method: (1) the standard procedure; (2) considering only trajectories I and III and (3) considering only trajectory I

6. Suggestions for practical application

Correction factors can be derived based on validated numerical models. Since it is concluded from this research that (I) the characteristic resistance of the individual layers, (II) the layer thicknesses relative to the cone diameter and (III) the number of layers within the zone of influence of the cone all affect the measured cone resistance, these aspects should be incorporated in a correction method that can be applied in engineering practice. In literature, correction factors are given as function of normalized layer thickness only, not taking into account the ratio of the characteristics of the individual layers. A possible method, which takes into account this ratio, is given in Figure 22. Based on the layer thickness and the ratio between the maximum resistance measured in a thin sand layer and the minimum resistance measured in the thin surrounding clay layers a correction factor for the thin sand layer is given. The two lines presented were derived using the Dutch method for the two tested layer configurations (H/d_{cone} ratio of 0.8 and 3.2 and sand and clay layers were of equal thickness). The line representing a H/d_{cone} ratio of 3.2 is derived based on the adapted method, as described above, which considers the average cone resistance over trajectory I only. Other lines (for other H/d_{cone} ratios) could be derived from additional investigations.

Figure 22: Example of a possible method to correct the measured cone resistance in thinly inter-layered soil deposits

It can be concluded from this research that limited contrast between the cone resistance of the sand and the clay layers will be seen in thin layers (low H/d_{cone} ratios). This will cause uncertainty applying a correction factor: a relatively small difference has relatively large consequences. The use of small cone diameters will reduce the uncertainty. The standard cone has not been developed to deal with thin layers, so in order to determine the layer thickness in the field, boreholes should be undertaken with detailed logging of recovered undisturbed samples. Also, a high measuring frequency during CPT is recommended to obtain a sufficient level of detail.

7. Discussion

It should be noted that the penetration rate applied in the experiments (4 mm/s) differs from the standard rate applied in the field (20 mm/s). Furthermore, the cone resistance has not been

corrected for the measured pore pressures. However, the effects of both these aspects are considered to be marginal.

Local variation in void ratio was observed in the artificially constructed soil samples, since it was hard to control the density index during preparation of saturated layered samples. This aspect was recognized and is taken into account in analysis of the test results.

The obtained correction factors do not necessarily apply to soils which experience higher in situ stress levels, since the tests presented in this paper are shallow CPTs. The tested multi-layered samples contained sand and clay layers of equal thickness, however, this is certainly not always the case in the field. Therefore, the presented correction factors cannot simply be applied to all thin layer deposits. Furthermore, only one density index of the interbedded sand layers and one type of clay was applied for preparation of the inter-layered samples. To achieve a sufficient database in order to validate a numerical method, a comprehensive test program should be performed investigating the effects of: (I) stress level, (II) density index and (III) layer configuration.

8. Summary and conclusions

This paper presents the results of a feasibility study to propose a correction method for determination of more realistic engineering properties of thin sand layers within thinly inter-layered soils. Thin layers are defined as layers which have a smaller thickness than the diameter of the penetrometer. CPT has been performed in artificial deposits containing multiple soil layers. Two different layer thicknesses were investigated. The test results were compared with existing analytical methods.

The experimental test set-up is suitable to investigate multiple thin layer effects on the cone resistance. The cone resistance in thinly inter-layered clay and sand deposits approaches a value slightly higher than the characteristic resistance of the clay layers. Correction factors for the interbedded thin sand layers (H/d_{cone} =0.8) above 1.5 are found, whereas factors below 1.5. are found for thicker sand layers (H/d_{cone} =3.2).

The elastic method of Vreugdenhil et al. (1994) seems to be unsuitable for very thinly layered soil deposits, while the Dutch method seems to be able to simulate the cone resistance in such deposits more accurately. It is thought that the mechanism in deposits containing multiple thin layers differs from deposits containing multiple thicker layers, since a different approach is needed to simulate the measurements properly.

It is concluded that (I) the characteristic resistance of the individual layers, (II) the layer thicknesses relative to the cone diameter and (III) the number of layers within the zone of

influence of the cone affect the cone resistance in deposits containing multiple thin soil layers. Suggestions for practical implementation are given.

Acknowledgements

The authors would like to acknowledge F.J.M. Hoefsloot and Fugro for their expertise, and use of the cone and data acquisitioning system. The supervision of M.A. Hicks, A. Askarinejad and R. Stoevelaar is very much appreciated, as well as the help of F.M. Schenkeveld and R. Zwaan during the physical testing.

References

Ahmadi MM (2000) Analysis of cone tip resistance in sand. Ph.D. thesis, University of British Columbia, Vancouver, B.C., Canada.

Ahmadi MM and Robertson PK (2004) Calibration chamber size and boundary effects for CPT qc measurements. In *Proceeding of ISC-2 on Geotechnical and Geophysical Site Characterisation*. Millpress, Rotterdam, The Netherlands, pp. 829-833.

Ahmadi MM and Robertson PK (2005) Thin-layer Effects on the CPT qc Measurement. Canadian Geotechnical Journal **42**:1302-1317, http://dx.doi.org/10.1139/t05-036.

Arshad M, Tehrani F, Prezzi M et al. (2014) Experimental study of cone penetration in silica sand using digital image correlation. Géotechnique **64(7)**:551-569, http://dx.doi.org/10.1680/geot.13.P.179.

Baldi G, Bellottti R, Ghionna M et al. (1986) Interpretation of CPTs and CPTUs. 2nd Part: Drained penetration of sands. In *Proceedings 4th International Geotechnical Seminar, Field Instrumentation and In-Situ Measurements*, pp. 143-155.

Bolton MD, Gui MW, Laue J et al. (1999) Centrifuge cone penetration tests in sand. Géotechnique **49(4)**: 543-552, http://dx.doi.org/10.1680/geot.1999.49.4.543.

De Lange DA, Van Beek VM, Schenkevel FM et al. (2016) Preparation techniques for unconventional sand samples. In *Proceedings of the 3rd European Conference on Physical Modelling in Geotechnics (EUROFUGE 2016)*, Nantes, France, pp. 61-66.

De Beer EE (1963) The Scale Effect in Transportation of the Results of deep sounding tests on the Ultimate Bearing Capacity of Piles and Caissons. Géotechnique **13(1)**:39-75, http://dx.doi.org/10.1680/geot.1963.13.1.39.

Emmett KB (2005) Pile disturbance in layered ground. Ground Engineering **38(12)**:30-32.

Hird CC, Johnson P and Sills GC (2003) Performance of miniature piezocones in thinly layered soils. Géotechnique **53(10)**:885-900.

Idriss IM and Boulanger RW (2008) Soil liquefaction during Earthquakes. Monograph EERI MNO-12, Earthquake Engineering Research Insitute, Oakland, CA, USA.

Joer HA, Randolph MF and Liew YH (1996) Interpretation of Cone Resistance in Layered Soils. In *Proceedings 7th Australia New Zealand Conference on Geomechanics* (Jaska MB, Kagawa WS and Cameron DA (eds)). Institution of Engineers, Australia, pp. 92-97.

Liao SSC and Whitman RV (1986) Overburden Correction Factors for SPT in Sand. Journal of Geotechnical Engineering **112(3)**:373-377, http://dx.doi.org/10.1061/(ASCE)0733-9410(1986)112:3(373).

Lunne T, Robertson PK and Powell JJM (1997) Cone Penetration Testing in Geotechnical Practice. First edition, Blackie Academic & Professional, ISBN 0751403938.

Martin AJ (2000) Flaser and wavy bedding in ephemeral streams: a modern and ancient example. Sedimentary Geology **136**:1-5, http://dx.doi.org/10.1016/S0037-0738(00)00085-3.

Meyerhof GG (1951) The Ultimate Bearing Capacity of Foundations. Geotechnique **2(4)**:301-332, http://dx.doi.org/10.1680/geot.1951.2.4.301.

Młyranek Z, Gogolik S and Półtorak J (2012) The effects of varied stiffness of soils layers on interpretation of CPTU penetration characteristics. Archives of Civil and Mechanical Engineering **12**:253-264, http://dx.doi.org/10.1016/j.acme.2012.03.013.

Mo PQ (2014) Centrifuge Modelling and Analytical Solutions for the Cone Penetration Test in Layered Soils. Ph.D. thesis, The University of Nottingham, Nottingham, UK.

Mo PQ, Marshall AM and Yu HS (2015) Centrifuge modelling of cone penetration tests in layered soils. Géotechnique **65(6)**:468-481, https://doi.org/10.1680/geot.14.P.176.

Mo PQ, Marshall AM and Yu HS (2017) Interpretation of Cone Penetration Test Data in Layered Soils Using Cavity Expansion Analysis. Journal of Geotechnical and Geoenvironmental Engineering **143(1),** ISSN 1943-5606, https://doi.org/10.1061/(ASCE)GT.1943-5606.0001577.

Prandtl L (1921) Über die Eindringungsfestigkeit Plastischer Baustoffe und die Festigkeit von Schneiden. Zeitschrift für Angewandte Mathematik und Mechanik **1**:431-436.

Reineck HE and Wunderlich F (1968) Classification and origin of flaser and lenticular bedding. Sedimentology **11**:99-104, http://dx.doi.org/10.1111/j.1365-3091.1968.tb00843.x.

Robertson PK (1990) Soil classification using the cone penetration test. Canadian Geotechnical Journal **27(1)**:151-158.

Robertson PK and Fear CE (1995) Liquefaction and its evaluation. In *Proceedings First International Conference on Earthquake Geotechnical Engineering* (Ishihara ed.), Balkema, Rotterdam, pp. 1253-1289.

Schmertmann JH (1978) Guidelines for cone rest, performance and design. U.S. Federal Highway Administration, report no. FHWATS-78209.

Senders M (2010) Cone resistance profiles for laboratory tests in sand. In *Proceedings 2nd International Symposium on Cone Penetration Testing*, Huntington Beach, CA, USA.

Silva M and Bolton MD (2004) Centrifuge penetration tests in saturated layered sands. In *Proceedings ISC-2 on Geotechnical and Geophysical Site Characterization* (Viana da Fonseca and Mayne (eds)), Millpress, Rotterdam, pp. 337-384.

Treadwell DD (1976) The influence of gravity, prestress, compressibility, and layering on soil resistance to static penetration. Ph.D. thesis, University of California at Berkeley, Berkeley, CA, USA.

Van den Berg P (1994) Analysis of soil penetration. Ph.D. thesis, Delft University of Technology, Delft, The Netherlands.

Van den Berg P, De Borst R and Huétink H (1996) An Eulerian Finite Element Model for Penetration in Layered Soil. International Journal for Numerical and Analytical Methods in Geomechanics **20**:865-886.

Van der Linden TI (2016) Influence of multiple thin soft layers on the cone resistance in intermediate soils. M.Sc. thesis, Delft University of Technology, Delft, The Netherlands, uuid:756ae85e-c1a2-4d3e-b070-5f237d521699.

Vreugdenhil R, Davis R and Berrill J (1994) Interpretation of Cone Penetration Results in Multilayered Soils. International Journal for Numerical and Analytical Methods in Geomechanics **18**:585-599, http://dx.doi.org/10.1002/nag.1610180902.

Walker J and Yu HS (2010) Analysis of the cone penetration test in layered clay. Géotechnique **60(12)**:939-948, http://dx.doi.org/10.1680/geot.7.00153.

Xu X (2007) Investigation of the End Bearing Performance of Displacement Piles in Sand. PhD thesis, The University of Western Australia.

Xu X and Lehane M (2008) Pile and penetrometer end bearing resistance in two-layered soil profiles. Géotechnique **58(3)**:187-197, http://dx.doi.org/10.1680/geot.2008.58.3.187.

Youd TL and Idriss IM (2001) Liquefaction Resistance of Soils: Summary Report from the 1996 NCEER and 1998 NCEER/NSF Workshops on Evaluation of Liquefaction Resistance of Soils. Journal of Geotechnical and Geoenvironmental Engineering **127(4)**:297-313, http://dx.doi.org/10.1061/(ASCE)1090-0241(2001)127:4(297).

Figures

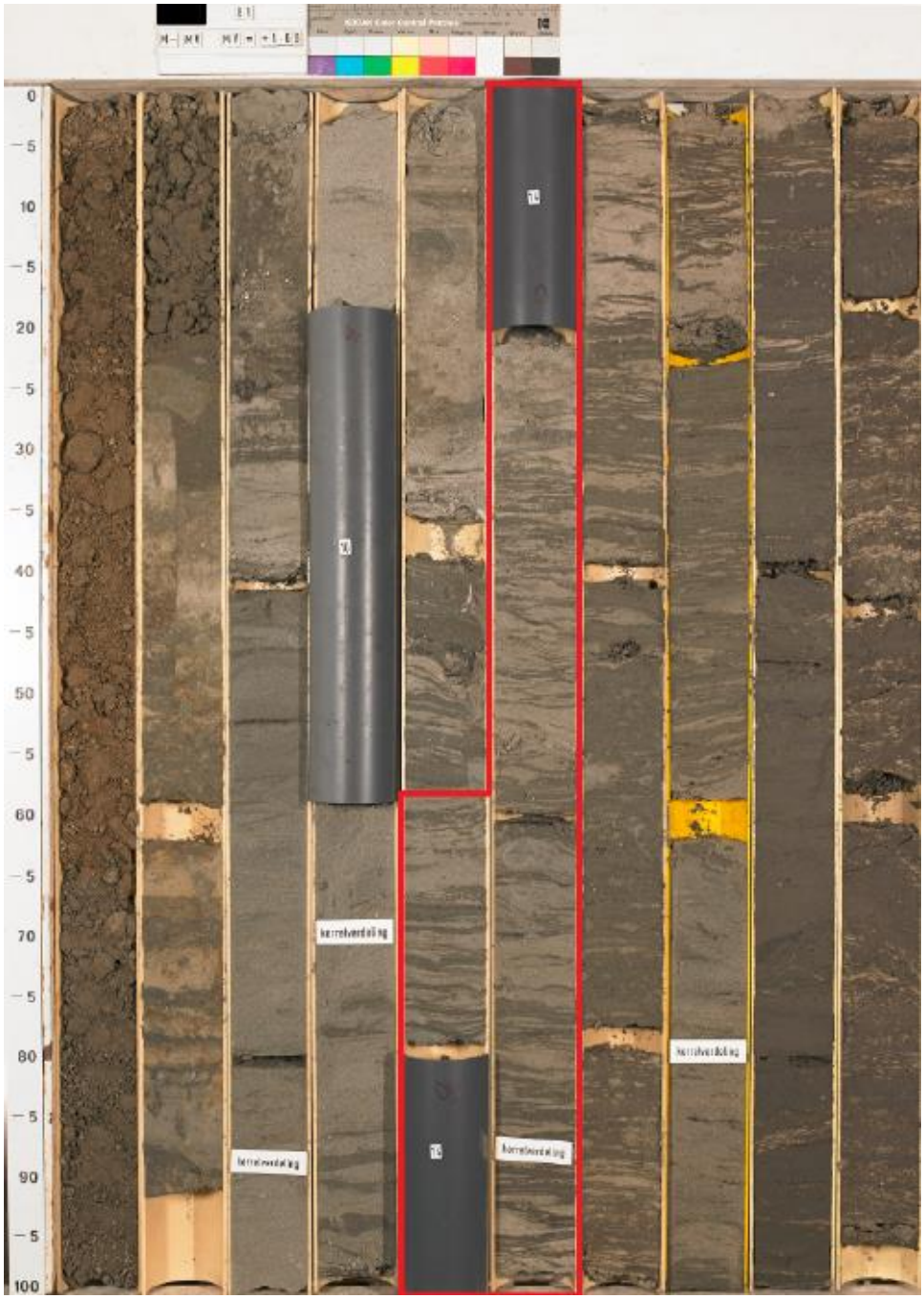

Figure 1: Sediment core with flaser bed sedimentation between depths of 4.5 m and 6 m marked in red (vertical scale in cm)

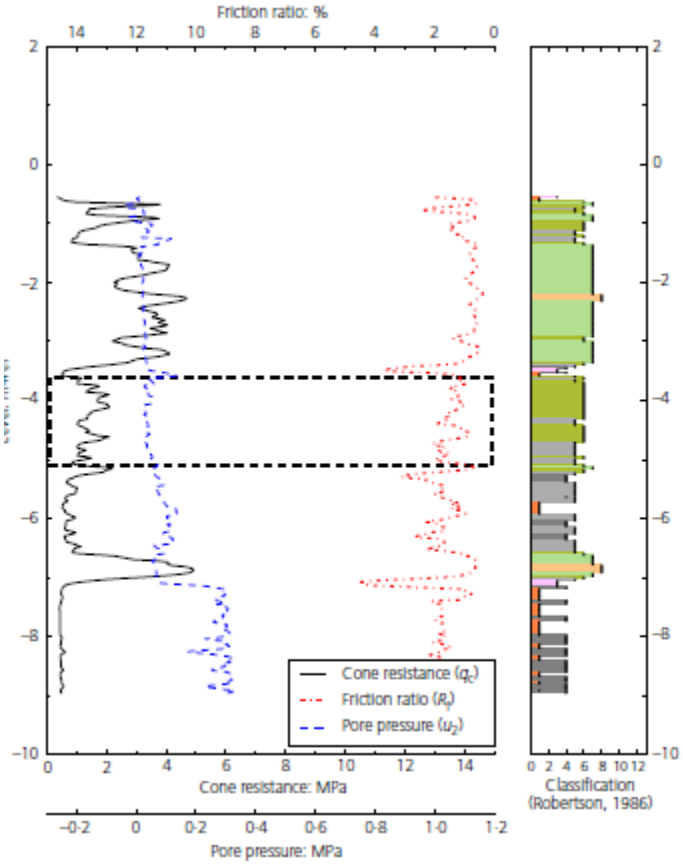

Figure 2: Example of cone penetration results in flaser beds undertaken close to the sediment core shown in Figure 1

Figure 3: Test set-up (steel tank with sand sample, Test 7)

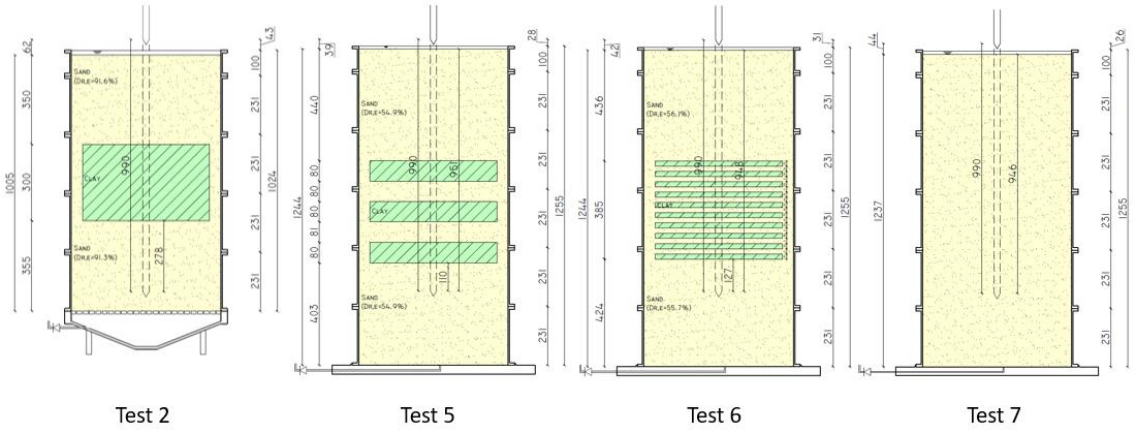

Figure 4: Test configurations: (a) Test 2, (b) Test 5 and (c) Test 6

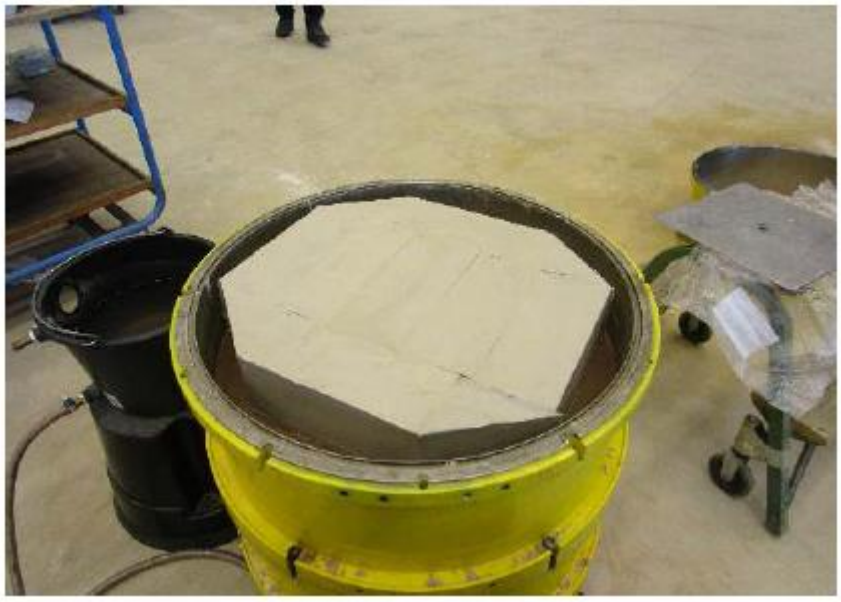

Figure 5: Preparation of clay layers for Test 2

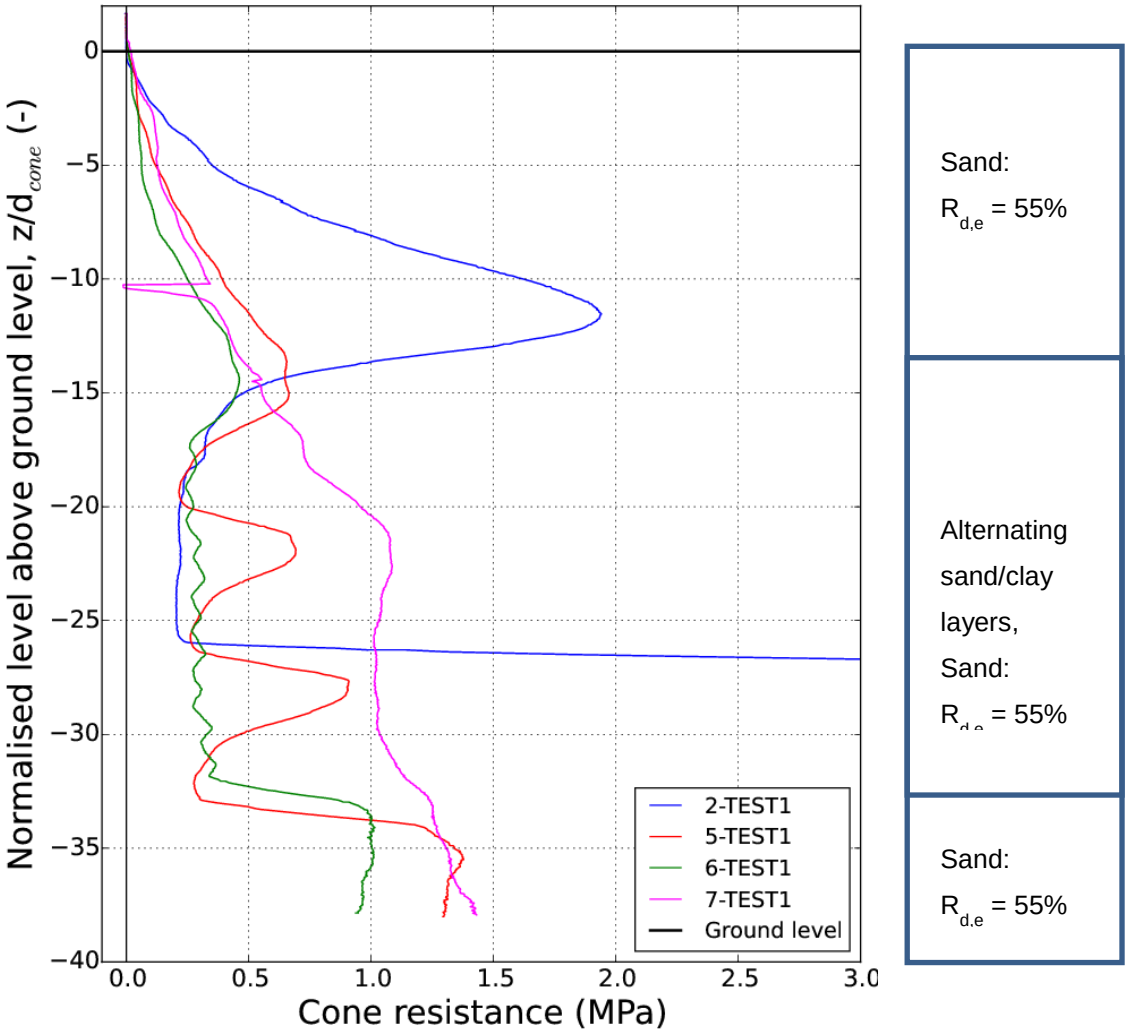

Figure 6: Measured cone resistances; note: I_D = 92% for Test 2, 55 % for the other tests

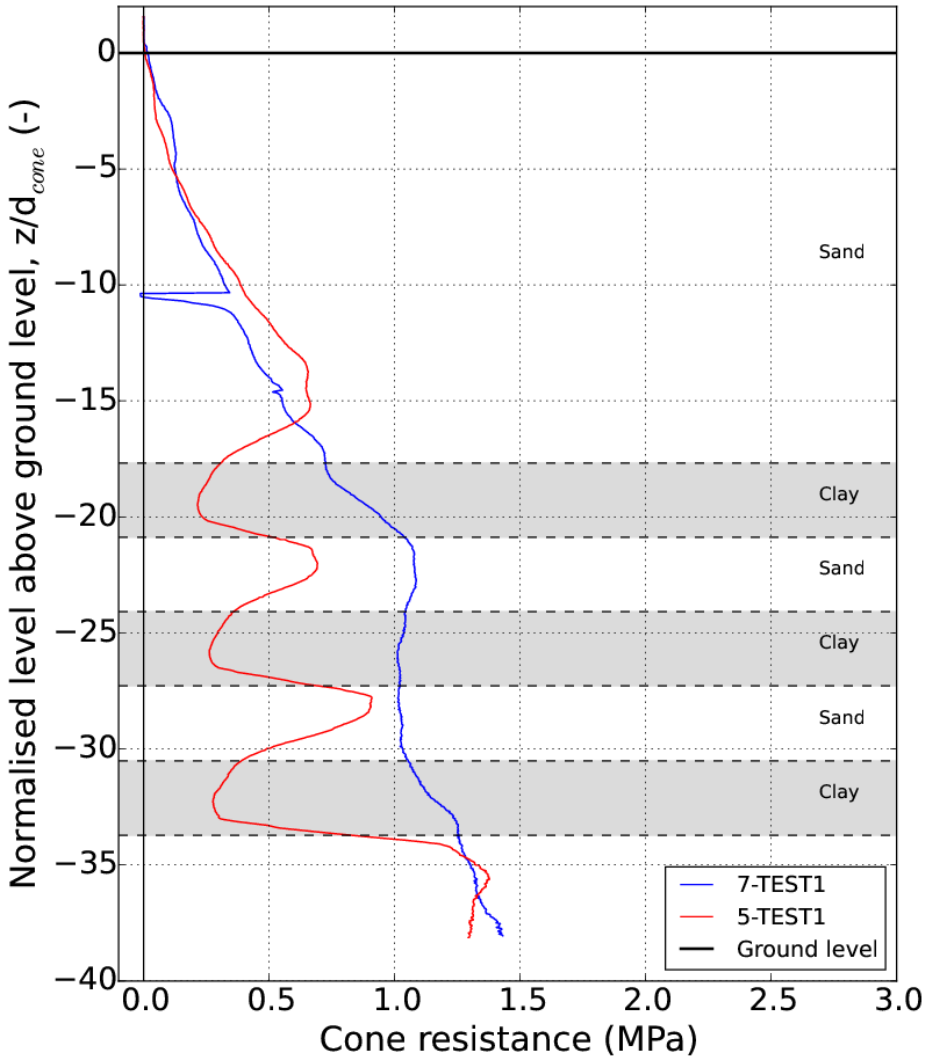

Figure 7: Cone resistance results for Test 5 in layered system (three clay layers, each 80 mm thick) compared with Test 7 (reference test, sand only)

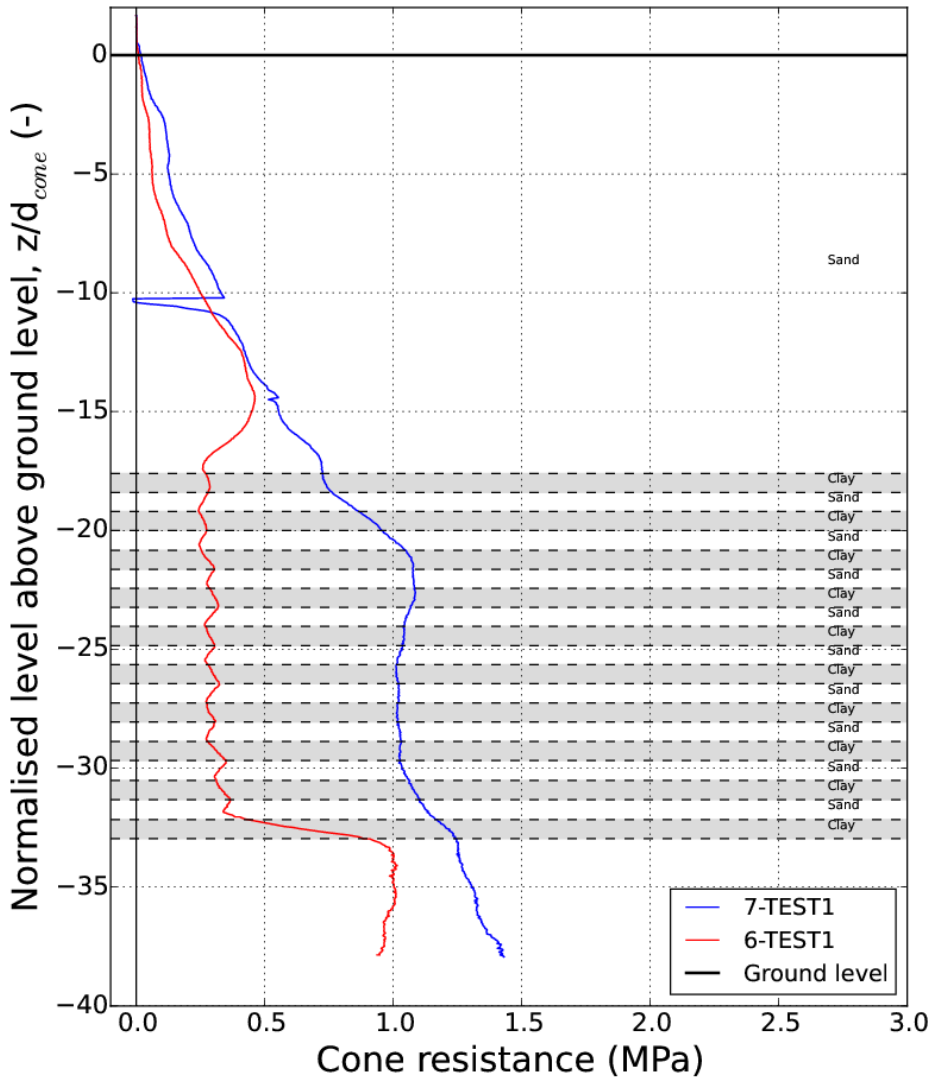

Figure 8: Cone resistance results for Test 6 in layered system (ten clay layers, each 20 mm thick) compared with Test 7 (reference test, sand only).

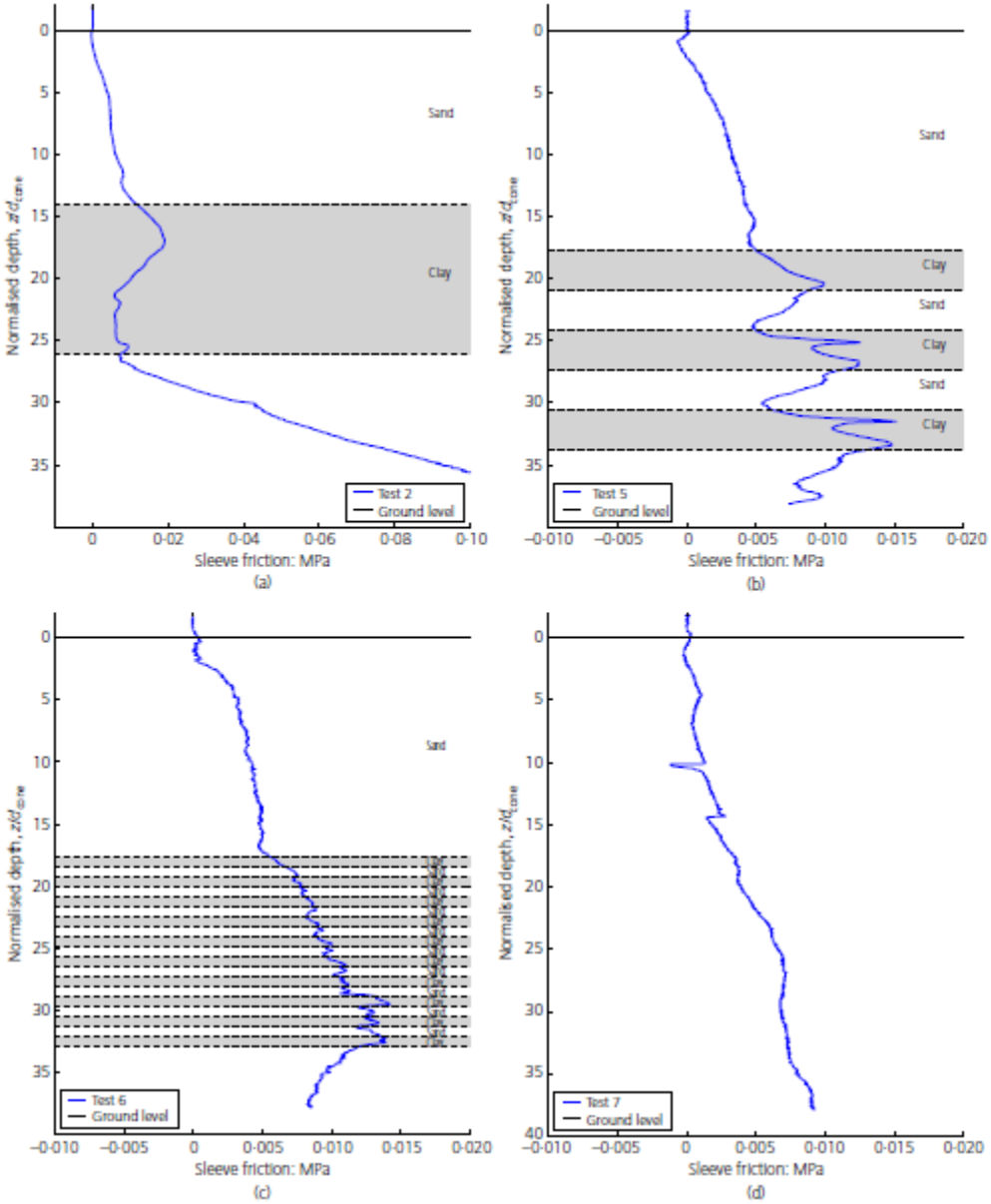

Figure 9: Results of friction sleeve measurements: (a) Test 2 (30 cm clay layer); (b) Test 5 (three clay layers, each 80 mm thick); (c) Test 6 (ten layers, each 20 mm thick); (d) Test 7 (sand only)

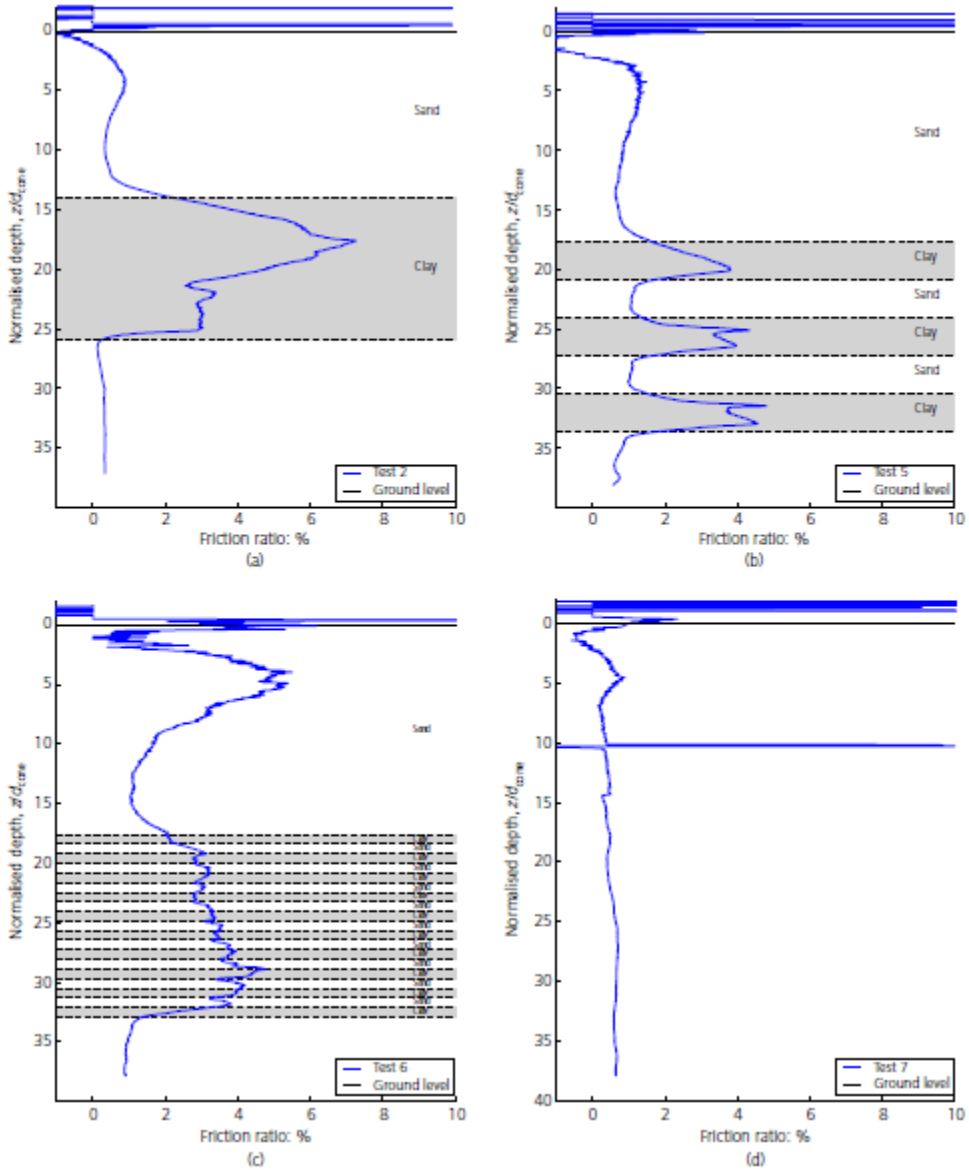

Figure 10: Friction ratio results: (a) Test 2 (30 cm clay layer); (b) Test 5 (three clay layers, each 80 mm thick); (c) Test 6 (ten layers, each 20 mm thick); (d) Test 7 (sand only)

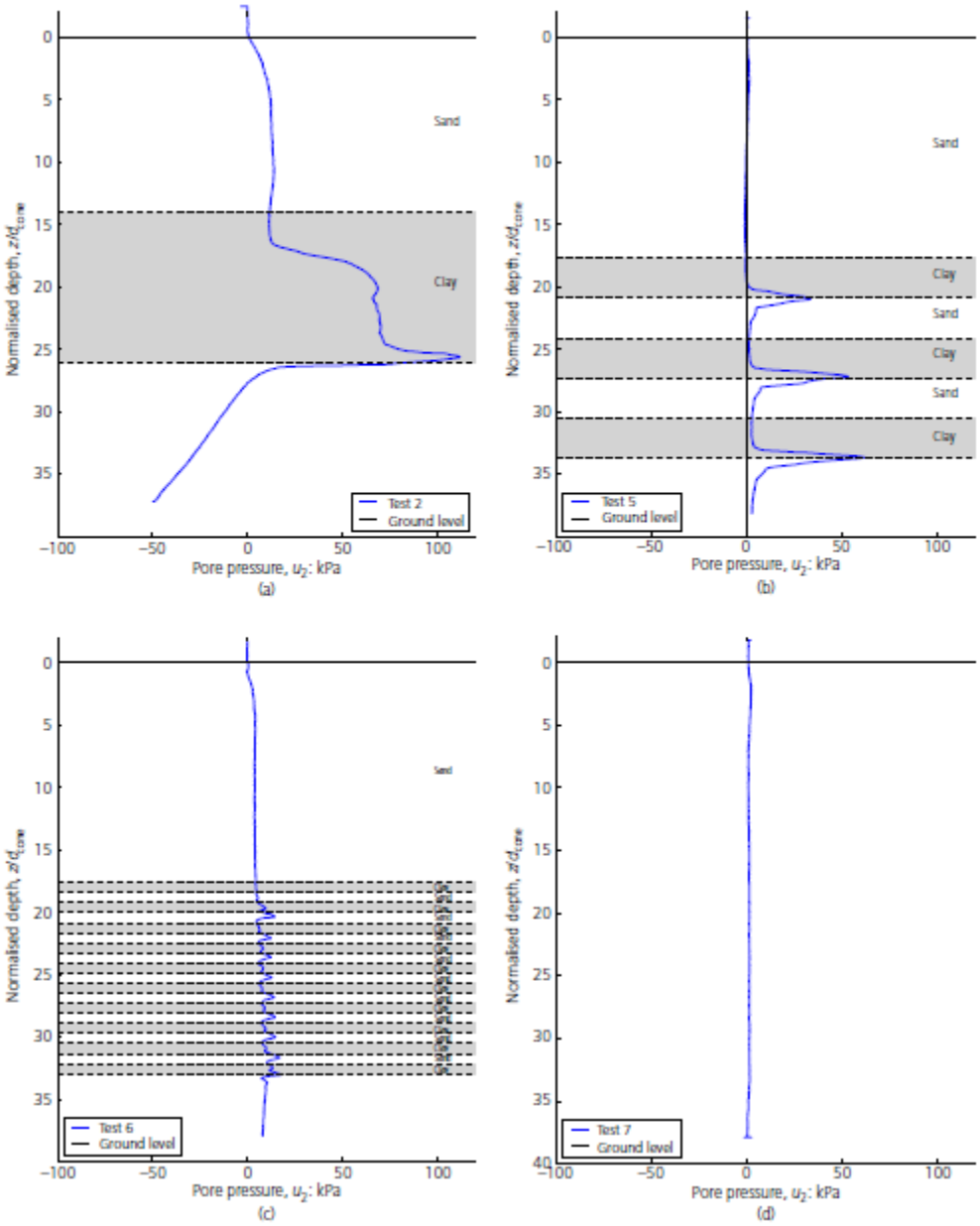

Figure 11: Results of pore pressure measurements: (a) Test 2 (30 cm clay layer); (b) Test 5 (three clay layers, each 80 mm thick); (c) Test 6 (ten layers, each 20 mm thick); (d) Test 7 (sand only)

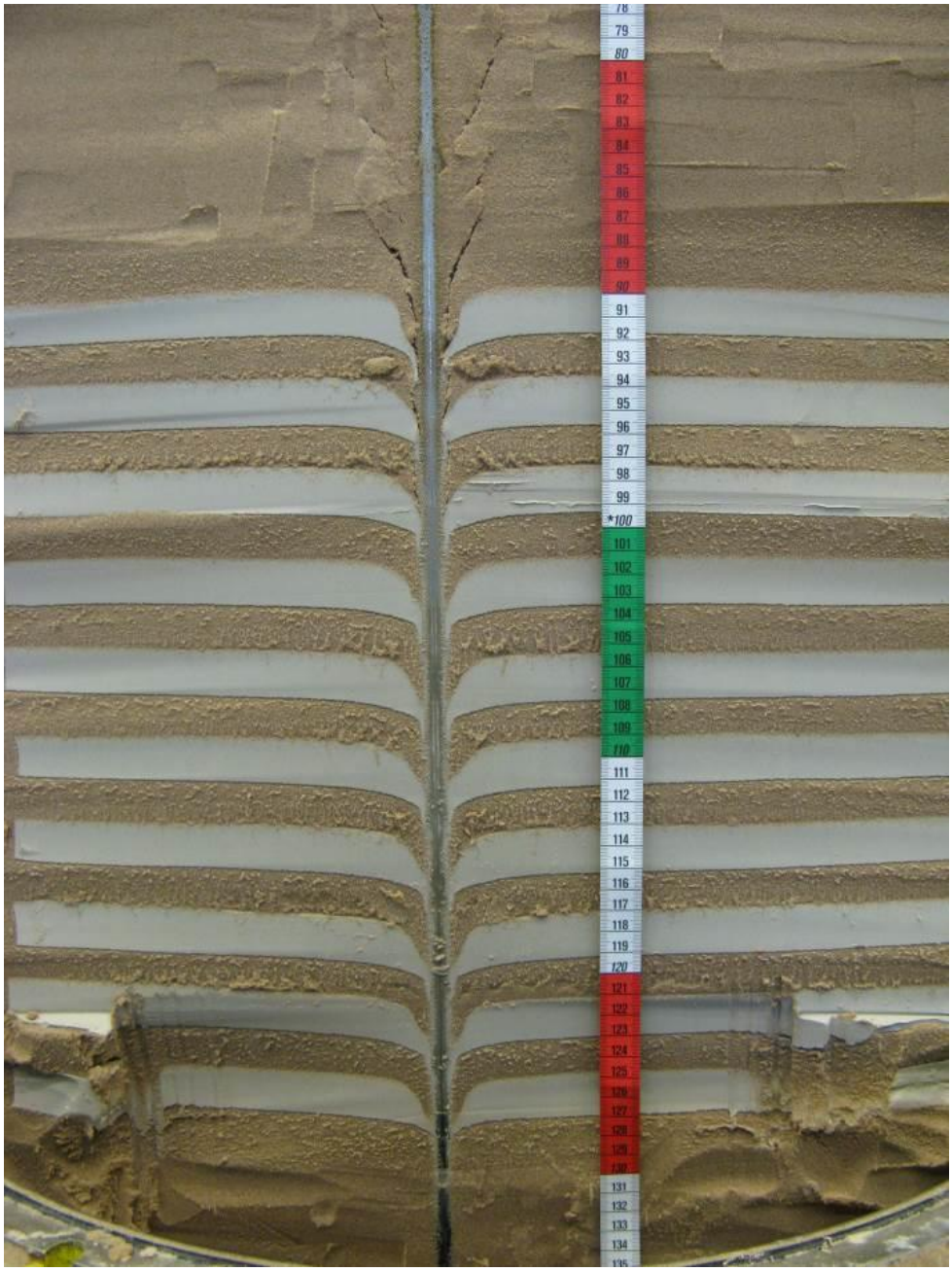

Figure 12: Excavation along the cone rod after completion of (a) Test 5 and (b) Test 6

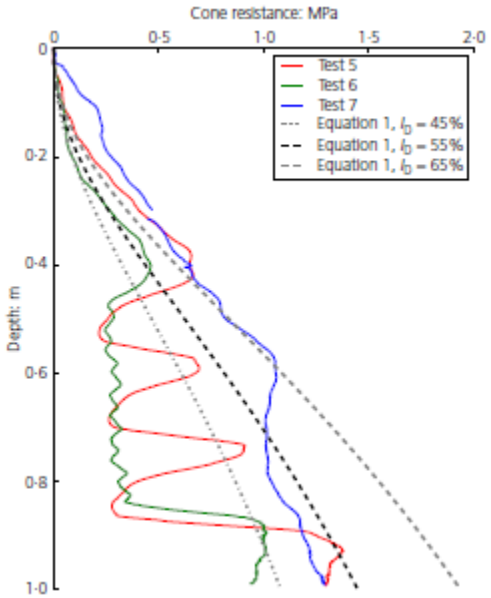

Figure 13: Characteristic cone resistances based on Lunne et al. (1997) and Senders (2010) for sands with density index of 45%, 55% and 65% respectively. The results of Tests 5, 6 and 7 are presented as well (dashed lines)

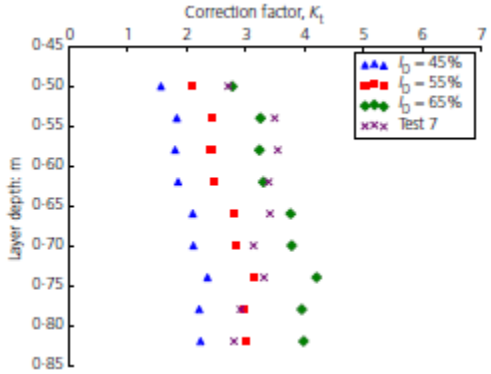

Figure 14: Correction factors derived for Test 6, multiple values of the characteristic cone resistance are used to account for the observed local variation in density index

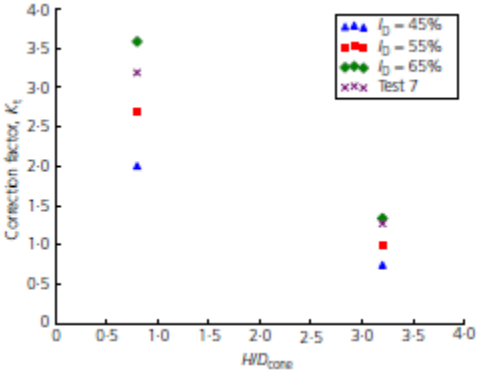

Figure 15: Average of derived correction factors Kt as function of the normalized layer thickness H/d_{cone}, multiple values of the characteristic cone resistance are used to account for the observed local variation in density index

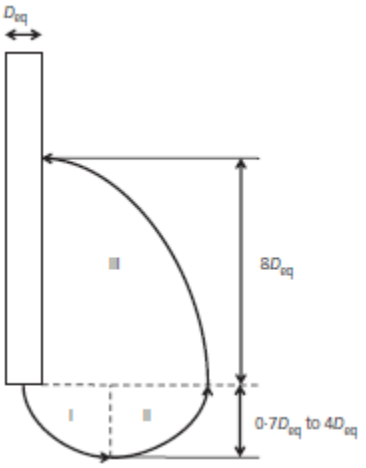

Figure 16: Schematic of the trajectories applied in the Dutch method

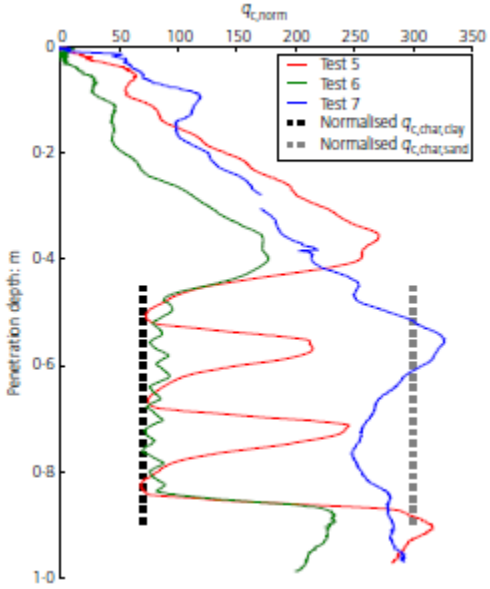

Figure 17: Test results normalized for the stress level with characteristic values for clay and sand (dashed lines)

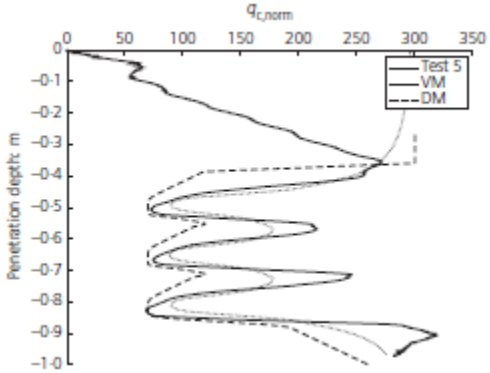

Figure 18: Simulations of Test 5

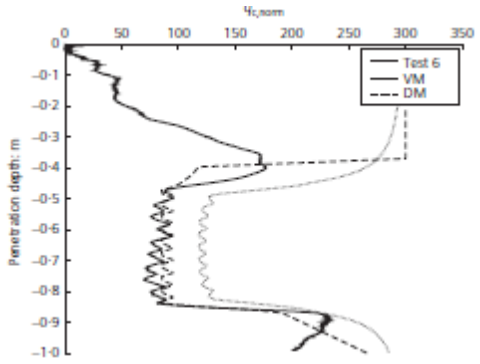

Figure 19: Simulations of Test 6

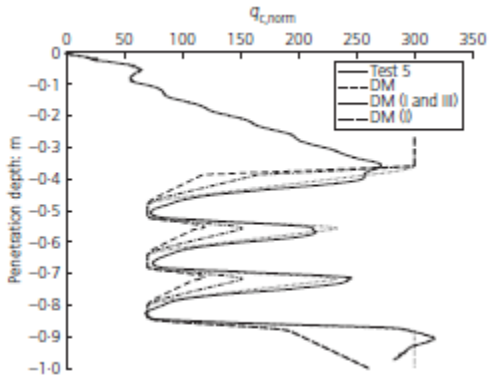

Figure 20: Simulations of Test 5 by three variants on the Dutch method: (1) the standard procedure; (2) considering only trajectories I and III and (3) considering only trajectory I

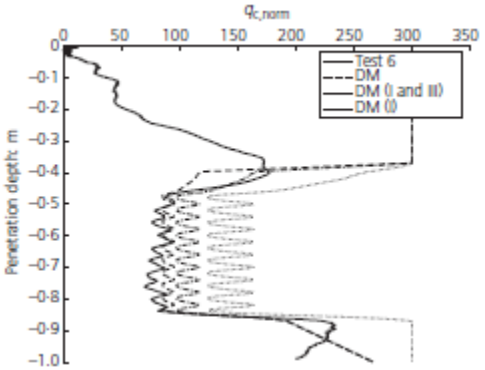

Figure 21: Simulations of Test 6 by three variants on the Dutch method: (1) the standard procedure; (2) considering only trajectories I and III and (3) considering only trajectory I

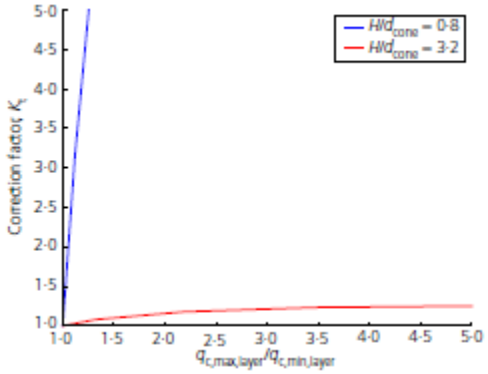

Figure 22: Example of a possible method to correct the measured cone resistance in thinly inter-layered soil deposits

Tables

Table 1: Sample properties of the relevant tests

Sample nr.	Layering	$R_{d,e}$ (sand)
2-TEST1	One 30 cm clay layer	92%
5-TEST1	Three 80 mm clay layers	55%
6-TEST1	Ten 20 mm clay layers	55%
7-TEST1	No layering	55%

Table 2: Characteristics of Baskarp sand

	d_{50} [-]	d_{60}/d_{10} [-]	min-max void ratio [-]
Baskarp sand	0.151	1.5	55.3% - 89.0%

Table 3: Characteristics of Vingerling clay

	Su [kPa]	WC [-]	PI [-]
Vingerling clay	15	24%	17%